Published in final edited form as:
J Control Release. 2013 March 10; 166(2): 159–171. doi:10.1016/j.jconrel.2012.12.002.

Stability of whole inactivated influenza virus vaccine during coating onto metal microneedles

Hyo-Jick Choi[a,b], **Brian J. Bondy**[a], **Dae-Goon Yoo**[c,d], **Richard W. Compans**[c], **Sang-Moo Kang**[c,e], and **Mark R. Prausnitz**[a,*]

[a]School of Chemical and Biomolecular Engineering, Georgia Institute of Technology, Atlanta, GA

[b]School of Energy, Environmental, Biological and Medical Engineering, University of Cincinnati, Cincinnati, OH

[c]Department of Microbiology and Immunology, Emory University School of Medicine, Atlanta, GA

[d]Department of Infectious Disease, College of Veterinary Medicine, University of Georgia, Athens, GA

[e]Center for Inflammation, Immunity, & Infection and Department of Biology, Georgia State University, Atlanta, GA

Abstract

Immunization using a microneedle patch coated with vaccine offers the promise of simplified vaccination logistics and increased vaccine immunogenicity. This study examined the stability of influenza vaccine during the microneedle coating process, with a focus on the role of coating formulation excipients. Thick, uniform coatings were obtained using coating formulations containing a viscosity enhancer and surfactant, but these formulations retained little functional vaccine hemagglutinin (HA) activity after coating. Vaccine coating in a trehalose-only formulation retained about 40 – 50% of vaccine activity, which is a significant improvement. The partial viral activity loss observed in the trehalose-only formulation was hypothesized to come from osmotic pressure-induced vaccine destabilization. We found that inclusion of a viscosity enhancer, carboxymethyl cellulose, overcame this effect and retained full vaccine activity on both washed and plasma-cleaned titanium surfaces. The addition of polymeric surfactant, Lutrol® micro 68, to the trehalose formulation generated phase transformations of the vaccine coating, such as crystallization and phase separation, which was correlated to additional vaccine activity loss, especially when coating on hydrophilic, plasma-cleaned titanium. Again, the addition of a viscosity enhancer suppressed the surfactant-induced phase transformations during drying, which was confirmed by *in vivo* assessment of antibody response and survival rate after immunization in mice. We conclude that trehalose and a viscosity enhancer are beneficial coating excipients, but the inclusion of surfactant is detrimental to vaccine stability.

[*]To whom correspondence may be addressed. prausnitz@gatech.edu, (Phone: (404) 894-5135, Fax: (404) 894-2291) .

Competing interests: M.**R.P.** is an inventor of patents that have been licensed to companies developing microneedle-based products, is a paid advisor to companies developing microneedle-based products, and is a founder/shareholder of companies developing microneedle-based products. This potential conflict of interest has been disclosed and is being managed by the Georgia Institute of Technology and Emory University.

Keywords

Coated microneedle patch; Skin vaccination; Influenza vaccine stability; Coating formulation; Crystallization; Phase separation; Osmotic pressure

1. Introduction

Microneedle patches have been studied as a novel means to administer vaccines with increased immunogenicity and simplified logistics [1-3]. The increased immunogenicity is believed to be due to targeting antigen delivery to the skin, which has a rich population of antigen-presenting cells and extensive lymphatic drainage [4-8], The simplified logistics arise from the easy administration of the vaccine (potentially by minimally trained healthcare personnel or by patients themselves), avoidance of dangerous hypodermic needles and sharps disposal, and small package size to reduce storage, transportation and disposal volumes.

Most research on microneedle patches has emphasized the use of microneedles measuring hundreds of microns in length that are often made of metal and are coated with a vaccine formulation [9-13]. Upon insertion into skin, the vaccine formulation dissolves off the microneedles into the skin within minutes, after which the microneedle patch is removed and discarded. Vaccines are typically coated onto microneedles by applying a liquid formulation that rapidly dries onto the microneedle surface, leaving a thin, solid film of vaccine and coating excipients.

It is well known that biopharmaceuticals can be destabilized during a drying process [14]. Sophisticated chemical formulations and drying protocols have been developed to protect these sensitive compounds during drying by lyophilization and other methods. However, these methods often cannot be directly transferred to use during coating of microneedles because (i) added excipients must be compatible with the coating process, (ii) the total amount of excipients applied to the microneedles must be small (e.g., 1 mg per patch) and (iii) microneedle coatings air-dry quickly (within minutes), leaving little time to modulate drying conditions.

The goal of this study was to investigate the factors and mechanisms involved in influenza vaccine destabilization during the coating of microneedles, especially those associated with the coating drying process. From our study on the stability of influenza vaccine coated onto microneedles during long-term storage, we know that thermodynamic processes in the solid coating, such as crystallization and phase separation, play a major role in vaccine activity loss [15]. The tendency of disaccharides to crystallize, as well as the suppression of this process using polymers, has been discussed previously in the context of influenza vaccines [16]. We also found that the surface properties of the coated substrate have an effect on these processes. Finally, we further hypothesize that osmotic stress during the drying process may affect vaccine stability.

These processes are all influenced by the composition of the coating formulation. In our lab, we often coat microneedles using aqueous formulations containing a surfactant (e.g., poloxamer) to facilitate good wetting of the microneedle surface, a viscosity enhancer (e.g., carboxymethyl cellulose) to increase coating thickness and a disaccharide sugar (e.g., trehalose) to stabilize the vaccine during drying [17]. Trehalose has been widely used as a stabilizer of biomolecules under low water conditions [18]. However, trehalose, and any other solute present at high concentration, can also function as an osmolyte to generate osmotic stress on the vaccine during drying of the coating.

This study sought to determine how each of these excipients affects stability of a whole inactivated influenza virus vaccine. We therefore tested a number of different coating formulations with different concentrations of each excipient. Dried coatings were then characterized using a hemagglutination (HA) assay as a measure of antigen preservation *in vitro* to determine vaccine activity [19, 20], light microscopy and X-ray powder diffraction (XRD) to find evidence of crystallization or phase separation, stopped-flow light scattering (SFLS) to observe osmotic shrinking behavior of the virus, and transmission electron microscopy (TEM) to find structural damage to the virus. *In vivo* immunogenicity and challenge experiments were also carried out in mice to confirm vaccine activity levels.

2. Materials and methods

preparation of vaccine

Influenza A virus (A/PR/8/34) vaccine was prepared as described previously [21].

Coating formulation and in vitro vaccine stability tests

To identify initial vaccine destabilizing factors, influenza vaccine stability tests were performed on titanium (Ti) plates before being tested on Ti microneedles. This model has been used previously due to the simplified sample preparation and has been shown to be equivalent to coating on microneedles [15]. The coating formulation used in all experiments was composed of one or more of the following: trehalose-dihydrate (Sigma Aldrich, St. Louis, MO), carboxymethyl cellulose sodium salt (low viscosity, Sigma Aldrich; abbreviated as CMC), surfactant Lutrol® micro 68 (poloxamer, BASF, Mt. Olive, NJ; abbreviated as Lutrol), and inactivated A/PR/8/34 virus in sterile Dulbecco's phosphate buffered saline (DPBS, Mediatech, Manassas, VA; pH 7.4), containing KC1 (0.2 g/l), KH_2PO_4(0.2 g/l), NaCl (8 g/l), and Na_2HPO_4(1.15 g/l).

Washed Ti plates were prepared by cleaning sequentially with acetone, methanol and isopropanol (Sigma Aldrich). Plasma-cleaned Ti plates were prepared first by washing, as above, and then by plasma cleaning (PDC-32G, Harrick Plasma, Ithaca, NY) for 1 min at the maximum radio frequency level.

For each sample, 1 μl of DPBS containing inactivated A/PR/8/34 virus (1 μg of protein) was mixed with 1 μl of coating formulation composed of the trehalose-only, trehalose/CMC, trehalose/Lutrol, or trehalose/Lutrol/CMC at room temperature using a pipette tip on a 0.1 – 0.2 cm^2 spot on a Ti plate. If not otherwise specified, T, L, and C have been used to stand for trehalose, Lutrol, and CMC, respectively. Test formulations are abbreviated as T15, T15C0.25, T15C0.5, T15C1, T15L0.5, T15L1, and T15L2, where the number following each letter corresponds to the concentration of the excipient in the formulation (after mixing with vaccine) in w/v %. The vaccine-coated Ti plates were then air-dried at ambient conditions. The remaining activity of the virus was then assessed by measuring hemagglutination (HA) activity [15, 22].

X-ray diffractometry

X-ray diffraction (X'pert Pro Multi Purpose Diffractometer, PANalytical, Westborough, MA) (XRD) analysis was used to study structural changes of the vaccine-embedded coating on Ti plates during storage. The measurements were made in the θ-2θ mode using a bracket sample holder with a C-u Kα radiation (Cu Kα_1 = 1.54059 Å, Cu Kα_2 = 1.54442 Å) at room temperature. Data were collected at 2θ between 8° and 40° using a step size of 0.0084° and an acquisition time of 5 s per step. Samples were measured at 45 kV and 40 mA. X-ray powder diffraction patterns were analyzed using Jade 8 software (MDI Materials Data, Livermore, CA) and shown after background correction. Diffraction peaks were fitted to a

Gaussian profile. The degree of crystallinity was calculated by measuring the integrated peak areas [23].

Viscosity and contact angle measurements

To investigate the effects of CMC and Lutrol on viscosity and hydrophobicity/wettability, 0, 0.25, 0.5 and 1% w/v of CMC and 0, 0.5, 1 and 2% w/v of Lutrol in 15% w/v of trehalose solution were prepared (unless otherwise noted, % w/v has been simplified as % to represent excipient concentration). Viscosity of the coating formulations was measured at room temperature using glass capillary viscometers following the manufacturer's protocol (Cannon Instrument, State College, PA). Wettability of the above coating solutions was compared by measuring contact angle on both washed and plasma-cleaned Ti plates. One microliter of the solution was dropped on a Ti plate and the contact angle was immediately measured from the analysis of an optical microscope image.

Osmotic shrinking kinetics of virus

Osmotic leakage properties of the inactivated A/PR/8/34 virus were analyzed by SFLS. The osmotic behavior of the virus was characterized by recording light scattering after a rapid mixing of inactivated A/PR/8/34 virus stock with an equal volume of a separate solution of trehalose-only, trehalose/CMC, trehalose/Lutrol, or trehalose/Lutrol/CMC in sterile DPBS. All osmolyte solutions were controlled to have 15% trehalose. Only the concentrations of CMC or Lutrol were varied in order to compare their effects on the osmotic shrinking behavior of the virus. Analysis was performed by stopped-flow spectrometry (MOS-200/M spectrometer, SFM-20; BioLogic Science Instruments) at a flow rate of 7 ml/s (injection volume 66 μl) at 4 °C. The excitation wavelength was set at 546 nm using a 150 W Xe light source and a monochromator (f/3.5 grating). The rate constant values (k) were obtained from a single exponential curve fitting of the light scattering spectra ($n > 30$) using Bio-Kine 32 V4.46 software (Bio-Logic).

Optical Microscopy and Electron microscopy

Morphological changes in the dried-vaccine coating on Ti plates and Ti microneedles were monitored using an optical microscope (SZX12, Olympus America, Center Valley, PA) with a CCD camera (RT Slider, Diagnostic Instruments, Sterling Heights, MI). A TEM (Hitachi-2000 FX, Hitachi High Technologies America, Schaumburg, IL) operated at 100 kV, was used to observe the morphology of the influenza vaccine. In preparation, a vaccine suspension was placed on a 3 mm formvar-amorphous carbon-coated copper grid (Ted Pella, Redding, CA) and allowed to settle for 3 min. Excess solution was removed by blotting with filter paper. Samples were then immediately stained with 1.5% phosphotungstic acid (pH = 7.0, Electron Microscopy Sciences, Hatfield, PA).

Water Content Measurement

The rate of water loss from the coating formulations was measured using an Aquatest coulometric moisture titrator (Photovolt Instruments, Minneapolis, MN) containing Karl Fischer Pyridine-free vessel solution. Data were collected after short-term drying (0 – 28 min) by preparing samples on a Ti plate and dissolving them in methanol. The dissolved samples were then injected into the titrator using a 1 ml airtight syringe (Hamilton Reno, NV). In some cases, samples were suspended directly into the titration vessel. Data were collected until the water detection rate fell to within 0.01 μg/min of the background rate.

Vaccine coating on microneedles

In vivo experiments were performed to evaluate the effects of excipients on vaccine stability using four different kinds of vaccine coatings on plasma-cleaned Ti microneedles:

inactivated virus coating with the T15, T15C1, T15L2, and T15L2C1 formulation. To compare the effects of the cleaning method on the vaccine activity, another group of vaccine-coated microneedles was prepared on washed Ti microneedles using the T15L2 formulation.

Ti microneedle arrays of five in-plane needles were fabricated by lithographic masking followed by wet etching [9], Each needle dimension was 750 μm in length, 50 μm in thickness and 200 μm in width at the base, which tapered to a sharp tip. Microneedles were cleaned using the same cleaning procedures as above for Ti plates. Microneedles were coated using an automated dip-coating apparatus [9], and air-dried at ambient conditions for 1 day before use. The amount of vaccine coated onto microneedles was determined by measuring the absorbance of vaccine samples dissolved off microneedles using a bicinchoninic acid (BCA) assay kit (ThermoFisher Scientific, Waltham, MA) at 560 nm on a microplate reader (iMark, Bio-Rad Laboratories, Hercules, CA).

Immunization and challenge of mice

Female inbred BALB/c mice (Harlan Laboratories, Indianapolis, IN) 6-8 weeks of age were each immunized once using influenza vaccine-coated microneedles (0.12 μg of total protein contents). Six groups of mice (6 mice per group) were tested: (1) naïve; plasma-cleaned microneedles coated with (2) T15, (3) T15C1, (4) T15L2, and (5) T15L2C1 formulation; (6) washed microneedles coated with a T15L2 formulation. Mice were challenged 4 weeks after immunization with a lethal dose of mouse-adapted A/PR/8/34 virus ($10\times LD_{50}$) to study survival rates and immune responses. Body weight changes of the mice were then monitored daily. Mice with a body weight loss greater than 25% were euthanized. Animal studies were approved by the Emory University and Georgia Tech Institutional Animal Care and Use Committees (IACUC).

Antibody responses

Serum samples were collected on the second week following immunization. Influenza virus-specific IgG antibodies were measured using enzyme-linked immunosorbent assay (ELISA) as described [24].

Statistics

All parameters were recorded for individuals within all groups. Data were analyzed by analysis of variance (ANOVA) and Student's t test. A *P*-value of less than 0.05 was considered to be significant. In some cases, median values were compared to validate the results.

3. Results

3.1. Functional activity of whole inactivated/live influenza vaccine coated on Ti plates

Our first experiments assessed the effect of coating formulation on the functional activity of influenza vaccine. Coating formulations contained different viscosity enhancer (CMC) and surfactant (Lutrol) concentrations. Functional hemagglutinin activity of the vaccine was assessed via HA assay after drying one day at ambient conditions. Plasma-cleaned Ti plates were used to simulate Ti microneedle surfaces to enable higher-throughput experimentation.

Drying influenza vaccine (either inactivated or live) with DPBS without excipient caused a dramatic loss of HA activity, down to 12.5% of pre-treatment values (data not shown). As shown in Fig. 1a, addition of 15% trehalose to the coating formulation retained much of the HA activity; 53% and 37% of pretreatment values was observed for inactivated and live virus vaccine, respectively. The addition of CMC to the formulation significantly increased

vaccine stability in a dose-dependant manner (one-way ANOVA, $P < 0.0005$) and approached 100% HA activity.

The effect of Lutrol in the formulation was more complex, as shown in Fig. 1b. Addition of a small amount of Lutrol (0.5%) increased vaccine stability relative to a trehalose-only formulation (Student's t-test, $P < 0.0005$). However, further increasing Lutrol concentration decreased HA activity in a dose-dependant manner (one-way ANOVA, $P < 0.0005$). This relationship may reflect competing effects of the Lutrol directly on the virus particles and indirectly through effects on the phase behavior or other properties of the trehalose matrix and/or Ti plate interface.

3.2 Morphological and microstructural behavior of coatings on Ti plates

To evaluate the possible role of physicochemical changes to the dried coating on vaccine activity, we examined morphological changes in vaccine coatings after one day of drying. Fig. 2a shows optical micrographs of representative coating samples on plasma-cleaned Ti plates. The coatings prepared from the trehalose-only (Fig. 2a(i)) and trehalose/CMC (Figs. 2a(ii)-(iv)) formulations appear morphologically similar. However, coatings prepared from the trehalose/Lutrol formulations (Figs. 2a(v)-(vii)) contained what appears to be phase separation, as evidenced by the formation of bumps (see insets in Fig. 2a). Moreover, the phase separation becomes clearer and more dominant as the Lutrol concentration increases, which is consistent with a previous report showing that the activity of the amphiphilic poloxamer (Lutrol) induced phase separation during drying processes [25]. The range of bump size was measured to be approximately 6 – 12 μm, 12 – 28 μm, and 30 – 50 μm for the formulations containing 0.5%, 1% and 2% Lutrol, respectively (Figs. 2a(v)-(vii)). Since no bumps were observed in the trehalose-only or trehalose/CMC formulations, it would appear that the Lutrol is responsible for these morphological changes during drying.

To better interpret these macroscale observations, we analyzed vaccine coatings using XRD for the same samples shown in Fig. 2a. Fig. 2b(i) displays XRD spectra measured from the trehalose-only and trehalose/CMC coating formulations. The broad halo peak observed at $2\theta = 10 – 30°$ represents the reflections from the amorphous phase, indicating that the coating matrix made of trehalose-only or trehalose/CMC remained amorphous.

In contrast, Fig. 2b(ii) shows that the trehalose/Lutrol formulations exhibited different phase behavior depending on Lutrol concentration. That is, XRD spectra revealed similar amorphous halo peaks from 0.5% Lutrol formulation, but crystalline peaks overlapping the amorphous halo peaks were observed with increasing intensity in the 1% and 2% Lutrol formulations. These peaks correspond to the characteristic peaks of crystallized trehalose dihydrate [26, 27]. As analyzed in Fig. S1 (in Supplemental Information), the addition of 1% and 2% Lutrol to trehalose solution generated 1.6 and 7.3% crystallization of the samples. The driving force for the phase separation and composition of each phase are not known. However, the increased crystallization seen by XRD in Fig. 2b appears to be associated with the phase separation seen by microscopy in Fig. 2a and likewise associated with the decreased HA activity with increasing Lutrol concentrations in Fig. 1b. This observation is consistent with our previous study showing an association between crystallization and influenza vaccine instability [15].

To better understand the kinetics of crystallization during drying of coatings, time-dependant XRD analysis was performed for representative trehalose-only, trehalose/CMC and trehalose/Lutrol formulations over the first 31 min of drying, as shown in Fig. 3. Consistent with the 24 h XRD data (Fig. 2b), the trehalose-only and trehalose/CMC formulations show an amorphous halo throughout the drying process (Figs. 3a-b). The broad peak at $2\theta = 28°$ present at 3 min is due to the high levels of water still present in the

coating. This peak quickly disappears as the water evaporates (Fig. S2). In the case of the trehalose/Lutrol formulation, the amorphous phase partially transforms into a crystalline phase within 10 min of drying (Fig. 3c). Moreover, the intensity of the crystal peaks of the coating increased with increased drying time.

3.3 Effects of Ti plate surface cleaning

Because phase changes often nucleate at interfaces and because surfactant is often most active at interfaces, we next examined the effect of changes in the cleaning process of the Ti substrate on which coatings were applied. The previous data came from Ti plates that were washed with organic solvents then plasma-cleaned; the next set of data comes from Ti plates just washed with organic solvents (see Materials and methods) without plasma cleaning (referred to as “washed plates”). We found that the functional HA activity losses of vaccine coated on washed Ti plates (Fig. 4) were, in many ways, similar to those seen on plasma-cleaned Ti plates (Fig. 1). The vaccine activity levels in trehalose-only and trehalose/CMC formulations were independent of Ti plate cleaning method (two-way ANOVA, $P = 0.28$). The vaccine activity levels for the low-concentration (0.5%) Lutrol formulation were also very similar (Student’s t-test, $P = 0.16$). However, unlike coatings on plasma-cleaned plates, increasing Lutrol concentration did not affect vaccine activity in coatings applied to washed plates. This suggests that the cleaning method used to remove surface contaminants has a significant effect on the stability of the coated influenza vaccine. The lower HA activity on plasma-cleaned plates compared to washed plates at the same Lutrol concentration implies the possibility of the vaccine-metal substrate interaction that enhances destabilization of influenza vaccine, in the case of plasma-cleaned Ti substrate (compare Fig. 4 with 1b).

To further evaluate the effects of metal substrate cleaning, changes in coating morphology were monitored on washed Ti plates by microscopy, as show in Fig. 5a. Similar to the plasma-cleaned Ti plates, Figs. 5a(i)-(iv) show coatings with no morphological changes in the trehalose-only and trehalose/CMC formulations. The trehalose/Lutrol formulation did show evidence of phase separation (Figs. 5a(v)-(vii)), but to a lesser extent and with smaller bumps (3 – 10 μm) compared to the same coatings on plasma-cleaned Ti plates (Figs. 2a(v)-(vii)). The time-dependant XRD spectra in Fig. 5b similarly show the formation of a crystalline phase on washed Ti plates, but to a lesser extent and with slower kinetics compared to plasma-cleaned Ti plates (Figs. 3c and S3). These results further support the contribution of reduced Lutrol-associated phase transformation, such as crystallization and phase separation, on washed Ti plates to retaining full HA activity of coated vaccines, in contrast to plasma-cleaned Ti plates.

3.4. Contact angle measurement

To better understand the efficiencies of different cleaning methods and their effects on the properties of the metal plate, we measured aqueous contact angles on washed and plasma-cleaned Ti plates to characterize the hydrophilicity of these surfaces. Representative images of contact angles from three coating formulations on these two surfaces are shown in Fig. 6a, and quantitative results from all seven formulations on both surfaces are shown in Fig. 6b. Regardless of coating formulation, the contact angles on washed Ti plates were much larger than those on plasma-cleaned Ti plates, suggesting that the process of washing produced a relatively hydrophobic surface, whereas plasma cleaning gave rise to a very hydrophilic surface. Surface wettability (i.e., the degree of surface energy and hydrophilicity) is a good indication of the amount of contamination by hydrophobic organic impurities [28], Therefore, contact angle measurements indicate that plasma cleaning is more effective at removing contaminants from the Ti surface than washing with organic solvents, consistent with previous findings [29].

Closer examination shows that on both surfaces, increasing CMC concentration weakly increased contact angle (two-way ANOVA, $P = 0.002$). Addition of Lutrol significantly lowered contact angle relative to the trehalose-only formulation (Student's t-test, $P < 0.000008$), but there was no additional significant effect on contact angle as a function of increasing Lutrol concentration (one-way ANOVA, $P = 0.35$). Notably, the contact angle was almost zero on plasma-cleaned Ti plate coated with the trehalose/Lutrol formulation, indicating an extremely hydrophilic surface. It is known that a 3-7 nm thick oxide layer is spontaneously formed on Ti surfaces due to the highly negative Gibbs free energy of formation [30, 31]. Thus, the physicochemical properties of Ti relevant in this study depend on this extremely thin titanium oxide film [32], Importantly, titanium oxide has been reported to have a high dielectric constant ($\boldsymbol{\varepsilon} \sim 114$) [33] as well as an isoelectric point in the range of 3.5-6.7 [34], indicating the presence of a negative surface charge upon exposure to a neutral aqueous solution, such as our coating formulation. As a result, the physicochemically reactive surface can lead to the adsorption of vaccine to the Ti substrate through electrostatic/hydrophobic interactions, similar to the adsorption of other biomolecules (e.g., peptides, proteins, lipids, and cells) to the metal surface [30, 32, 35, 39], Plasma cleaning could cause increased adsorption by removing contaminants and increasing the surface energy. Furthermore, the presence of Lutrol increases the wetting properties of the vaccine coating, which will increase the extent of vaccine-substrate interaction. This accounts for the correlation between the generation of hydrophilic surface and the decrease of vaccine activity in the presence of Lutrol. Therefore, enhanced destabilization of vaccine on the plasma-cleaned Ti surface is believed to be caused by adsorption of vaccine and/or conformational change of the vaccine through its interaction with the Ti substrate.

We have considered the effects of three design features of coatings on vaccine stability and associated phase transformations: viscosity enhancer (CMC), surfactant (Lutrol) and surface cleaning method. Plasma cleaning in combination with surfactants appears to cause an increased vaccine-substrate interaction. However, in the absence of Lutrol, no negative effects were seen with plasma cleaning. The addition of Lutrol on washed Ti surfaces helped stabilize the vaccine, but, in a separate study, we found that Lutrol was associated with phase transformation and vaccine instability during long-term (i.e., weeks to months) storage of influenza vaccine-coated microneedles [15]. For this reason, we next focused our analysis on identifying stabilizing effects of the viscosity enhancer CMC in the vaccine coating formulation.

3.5. Effects of formulation with both a viscosity enhancer and surfactant on vaccine stability

While CMC alone did not stabilize influenza vaccine during drying (data not shown), use of trehalose in addition to CMC increased vaccine activity with increasing CMC concentration (Figs, 1a and 4). Because surfactant is also needed to effectively coat microneedles [17], we next examined formulations composed of all three excipients (trehalose, CMC, and Lutrol) to understand their effects on vaccine.

Fig. 7 shows vaccine stability after drying in coating formulations composed of a constant level of Lutrol and trehalose and varying levels of CMC. Addition of low-concentration (0.5%) Lutrol to the trehalose formulation increased vaccine activity (Student's t-test, $P < 0.0005$), consistent with our previous data (Fig. 1b). Addition of CMC at varying levels had no further effect on vaccine activity (one-way ANOVA, $P < 0.0005$).

We next varied the Lutrol concentration while keeping CMC and trehalose concentration constant (Fig. 7). Increasing Lutrol concentration decreased vaccine activity in the presence of CMC and trehalose (one-way ANOVA, $P < 0.0005$). This is qualitatively consistent with our previous finding that increasing Lutrol concentration in the absence CMC also decreased

vaccine activity (Fig. 1b). However, quantitatively, vaccine activity was higher at elevated Lutrol concentration with CMC than that from formulation without CMC (two-way ANOVA, $P < 0.0005$). This shows that CMC reduced the damaging effects of high Lutrol concentration in the presence of trehalose.

Because vaccine activity loss in trehalose/Lutrol formulations on plasma-cleaned Ti plates was shown to be associated with phase transformations of the coating and interaction with the metal substrate, we hypothesize that the addition of CMC suppresses these phase transformations and vaccine-substrate interaction. The nucleation and growth of trehalose crystals and the phase separation processes are driven by the diffusion of excipients. Therefore, these results further suggest that CMC suppresses both Lutrol-induced phase transformations and vaccine-Ti plate interactions by increasing coating formulation viscosity and thereby retarding diffusion of excipients (see Fig. S4 for viscosity as a function of CMC and Lutrol concentrations).

3.6. Role of osmotic stress in coating formulations

In addition to phase transformations damaging vaccine activity, we also considered the role of osmotic forces on vaccine virus particles. Since the lipid envelope of the inactivated influenza virus functions as a diffusion barrier against solutes, vaccine can be subject to osmotic shocks in natural environment [40], To assess the effect of CMC and Lutrol on the osmotic pressure applied to the vaccine, the osmotic shrinking behavior of the inactivated virus was investigated using SFLS. Osmolyte solutions were controlled to have a final trehalose concentration equal to 15% and concentrations of CMC and Lutrol were varied to compare the effects of CMC and Lutrol on the osmotic shrinking behavior of the virus.

As a control experiment, the SFLS spectrum measured after rapid mixing of virus with the trehalose-only solution is shown in Fig. 8a. The SFLS signal exhibited a step-wise intensity increase over time (Fig. 8a(i)). Since an increase in intensity of the SFLS curve is related to a volumetric decrease, the trehalose-only solution is believed to have created hypertonic osmotic stress on the virus. We believe the first shrinkage at 0 s ($k \sim 1.0\ s^{-1}$, Fig. 8a(ii)) corresponds to the shrinkage of the viral envelop by increasing packing density of the membrane and the second shrinkage at 34 s (Fig. 8a(i)) indicates the resistance of the matrix protein (M1) to further shrinkage, although additional studies are needed to assess this.

Fig. 8b shows SFLS spectra performed on the virus in response to increasing CMC concentration at constant trehalose and Lutrol concentration. Because trehalose is present at a much greater concentration than the other two excipients, the concentration gradient-driven driving force for osmotic pressure is dominated by the trehalose. As shown in the spectra (Fig. 8b(i)), the virus experienced the previously observed step-wise osmotic shrinking behavior. We chose the onset time of the second shrinkage, t_{2nd}, to be a characteristic time of the shrinkage process, and found that it increased with increasing CMC concentration (one-way ANOVA, $P < 0.0005$), while the rate of primary shrinkage, denoted by the rate constant k, decreased with increasing CMC concentration (one-way ANOVA, $P < 0.0005$) (Fig. 8b(ii)). We interpret these data to mean that slower shrinkage is caused by decreased osmotic pressure, which is due to the heightened medium viscosity with the increase of CMC concentration. Osmotic pressure is known to be inversely related to the medium viscosity [41, 42] and its onset was delayed in the presence CMC (Fig. S4). Therefore, the CMC-induced stabilizing effect (Figs. 1a, 4, and 7) may be accounted for, in part, by the reduction in the drying-induced osmotic pressure to the virus.

The corresponding data are shown in Fig. 8c for the effects of increasing Lutrol concentration at constant trehalose and CMC concentration. There was a significant effect of Lutrol concentration on the osmotic shrinkage behavior of the virus for k but not t_{2nd} (one-

way ANOVA, $P < 0.0005$ for k and $P = 0.098$ for t_{2nd}). However, the tiny range of the overall variation between sample groups has no practical significance. Thus, the Lutrol-induced destabilization of the vaccine seen previously (Figs. 1b and 7b) may not be attributed to increased Lutrol-induced osmotic stress. Similarly, the vaccine stabilization seen at low Lutrol concentration may not be attributed to decreased Lutrol-induced osmotic stress either.

3.7. Morphological changes of dried influenza vaccine

To better understand effects of vaccine formulation on the inactivated virus particles after drying on plasma-cleaned Ti plates, morphological changes of the vims was compared before and after drying using TEM analysis (Fig. 9). As a positive control, the virus in DPBS is shown in Fig. 9a. The virus maintained its spherical shape and typical spike-shaped surface morphology due to its antigenic membrane proteins. When using low Lutrol concentration formulations with low- or high-concentration CMC, no morphological differences were seen between samples before (i) and after (ii) drying (Figs. 9b and c), which corroborates the lack of activity loss under these conditions, as shown in Fig. 7. However, virus particles dried using a high Lutrol concentration formulation also did not show morphological differences before and after drying, even though HA activity loss was seen under those conditions (Fig. 7). This suggests that the observed HA activity decrease during drying may be at the molecular level associated with denaturation of HA antigenic proteins, which cannot be visualized by TEM analysis.

3.8. Effect of vaccine formulation on coating of microneedles with vaccine-coated Ti microneedles applied to the skin

We next performed experiments using vaccine-coated Ti microneedles (700 μm long). Plasma-cleaned microneedles coated with trehalose-only (Fig. 10a) and trehalose/CMC (Fig. 10b) formulations had smooth morphology similar to that on plasma-cleaned Ti plates (compare with Figs. 2a(i) and (iv)). Plasma-cleaned microneedles coated with a trehalose/Lutrol formulation (Fig. 10c) exhibited extensive phase separation, similar to that observed on the plasma-cleaned Ti plate (Fig. 2a(vii)). However, bumps were mostly observed near the edge of the coating on Ti plate, but were uniformly distributed throughout the coating film on the microneedles. Coating with a trehalose/Lutrol formulation on washed Ti microneedles further increased phase separation, as evidenced by the formation of larger bumps (sized from 10 to 30 μm, as shown in Fig. 10d) compared to those on the washed Ti plate (Fig. 5a(vii)). Finally, the addition of CMC to the trehalose/Lutrol formulation on plasma-cleaned is shown in Fig. 10e. These needles showed a fairly smooth surface morphology that, despite wrinkled appearance, showed a lower density of phase separation bumps compared to the trehalose/Lutrol formulation in the absence of CMC (Fig. 10c).

3.9. Influenza-vaccine immunization with microneedles and protection against challenge

To confirm our *in vitro* findings, we performed *in vivo* experiments using mice vaccinated with Ti microneedles applied to the skin, and a non-vaccinated control. In addition to a naive, unvaccinated group, five groups of mice were vaccinated with microneedles coated with 0.12 μg of inactivated influenza virus vaccine: T15 (plasma-cleaned), T15C1 (plasma-cleaned), T15L2 (plasma-cleaned), T15L2 (wet-cleaned), and T15L2C1 (plasma-cleaned). A high Lutrol concentration was used to clearly show the effects of surfactants after one day drying.

3.9.1. Microneedle vaccination with viscosity enhancer is more immunogenic

—As Fig. 11 shows, immunization with trehalose-only or trehalose/CMC formulations generated strong antibody responses. In contrast, insignificant antibody production was

observed in the groups immunized with trehalose/Lutrol formulations prepared on either washed or plasma-cleaned microneedles. This is consistent with the findings that HA activity was reduced for this formulation on plasma-cleaned Ti surfaces *in vitro* (Fig. 1b) and that phase transformation were also associated with these formulations on both washed and plasma-cleaned surfaces (Figs. 2, 3c and 5). Immunization with the trehalose/Lutrol/CMC formulation generated high levels of antibody production, which is consistent with our observation that CMC suppresses the destabilizing processes caused by Lutrol and interaction between the vaccine and metal substrate (Fig. 10).

3.9.2. Microneedle vaccination with viscosity enhancer confers better protection—The five different groups of vaccinated mice and control mice were challenged after four weeks with a lethal dose of the mouse-adapted A/PR/8/34 influenza virus ($10\times LD_{50}$) to study post-challenge survival rates. As shown in Figs. 12a and b, the groups of mice vaccinated with microneedles coated with the trehalose/Lutrol formulation (both the washed and plasma-cleaned groups) and the negative control group all exhibited a rapid body weight loss followed by death within 8 days of challenge. This indicates that microneedles coated with the trehalose/Lutrol formulation cannot provide protection against lethal viral challenge. In contrast, 80% of the mice vaccinated with microneedles coated with the trehalose-only formulation survived challenge with approximately 15% peak body weight loss. However, the groups immunized by microneedles with CMC (both the trehalose/CMC and the trehalose/Lutrol/CMC formulations) were protected 100% against lethal challenge, which is consistent with the antibody response data as well (Fig. 11). This further confirms that inclusion of CMC in the formulations was associated with improved protective immunogenicity, probably due to increased vaccine stability by alleviating osmotic stress, suppression of phase separation, and reducing the affinity between vaccine and Ti plates.

4. Discussion

In this study, the stability of influenza vaccine-coated microneedles was investigated *in vitro* and *in vivo.* The purpose of this work was to identify vaccine destabilizing factors during the microneedle coating/drying process, investigate the role of excipients in the current microneedle coating formulation, and design a strategy to maintain protective efficacy of the vaccine during drying.

4.1. Trehalose

Disaccharides have been used often in microneedle coating formulations to protect the functional activity of vaccines from drying-induced damage [12], Guided by this previous work, this study used 15% trehalose in all coating formulations to take advantage of the sugar-induced stabilizing effect. No significant levels of functional HA activity were detected in coatings made from formulations composed of surfactant and/or viscosity enhancer without trehalose (data not shown). However, about 40 – 50% HA activity remained for vaccine in the trehalose-only coating formulation (Figs. 1a and 4). Despite this protective effect, vaccine activity was not 100% in the trehalose-only formulation, showing the need for further improvement. Incomplete protection of vaccine activity during drying may indicate osmotic pressure-induced viral deactivation.

4.2. Osmotic pressure

To better understand the effects of osmotic pressure on the inactivated virus vaccine, both HA activity changes and time-dependant osmotic shrinking behavior were monitored using HA titers and SFLS, respectively, in response to changes in the coating formulation. As demonstrated in Figs. 1a, 4, and 7, both live and inactivated viruses exhibited better stability

with increasing CMC content, either with or without the additional presence of Lutrol (Fig. 7). For the same coating formulations, SFLS analysis showed that the presence of CMC in the coating formulation resulted in a longer secondary shrinkage time (Fig. 8b), which indicates decreased osmotic stress. Increasing Lutrol concentration did not generate a meaningful level of osmotic pressure (Fig. 8c). Finally, increasing CMC concentration was also shown to increase coating formulation viscosity, whereas Lutrol had no effect (Fig. S4).

These data show that CMC increased viral stability, decreased osmotic stress and increased coating formulation viscosity. Taken together, these suggest that the increased viscosity imparted by CMC decreased osmotic stress, thereby reducing the destabilization of the virus by osmotic forces. While our data suggest this causative relationship, additional studies are needed to more fully test it.

It should also be mentioned that a higher CMC concentration (≥ 2%) in a trehalose/CMC formulation decreased HA activity (at 2% CMC, ~ 60% HA activity was observed). It is known that the degree of protection conferred by the sugar depends to a large extent on the amount of hydrogen bonding between the sugars and the lipid head groups and proteins [18]. It is possible that extremely high viscosity at such a high CMC concentration may interfere with the protective effect of trehalose on the vaccine by interfering with or retarding the formation of these bonds.

4.3. Crystallization of coatings

The crystallization of trehalose in the trehalose/Lutrol coating began very early in the drying process (10 – 14 min after drying. Figs. 3c and 5b). An explanation for this phenomenon can be constructed by looking at the formulation's glass transition temperature (T_g). It should be noted that obtaining actual measurements of T_g values for the coating formulations at 10 min would be prohibitively difficult, due to the long time needed to perform the measurements and the continuous evaporation of residual water in the sample during that time. Instead, the Gordon-Taylor equation was used to calculate T_g for the trehalose-water system [44],

$$T_g = \frac{\left(w_{sugar} \cdot T_{g(sugar)} + k \cdot w_{water} \cdot T_{g(water)}\right)}{\left(w_{sugar} + k \cdot w_{water}\right)}$$

where w_{sugar}, w_{water}, $T_{g(sugar)}$, and $T_{g(water)}$ represent the weight fractions (w) and the glass transition temperatures of sugar and water, respectively, and $k = 5.2$ [45, 46].

The water content change is shown as a function of time in Fig. S2. After 10 min of drying, the water content decreased to 17.3% and 19.8% of the original value on washed and plasma-cleaned Ti plates, respectively. Using reported T_g values of trehalose and water ($T_{g(trehalose)} = 115$ °C and $T_{g(water)} = -138$ °C [46, 47]), the T_g of the trehalose/Lutrol (T15L2) coating was calculated to be approximately −100 °C on the washed/plasma-cleaned Ti plates after 10 min of drying at ambient conditions. Although this value is lower than room temperature, it is important to note that this value indicates an increased nucleation potential, but not the crystallization rate. This can explain the non-crystallizing behavior of T15 during the early stage of the drying process (Figs. 2b(i) and 3a).

According to previous reports, the addition of poloxamer 188 (Lutrol) did not cause significant changes in the T_g of trehalose [25] or mannitol [48]. This indicates that the contribution of Lutrol to the T_g calculation can be neglected and, thus, the T_g for the trehalose/Lutrol formulations can be approximated as a binary mixture of water and

trehalose. In this calculation, phase separation was not considered; i.e., the coating was assumed to have a homogenous composition of trehalose and Lutrol. However, Lutrol-induced phase separation is accompanied by the likely formation of trehalose-rich and trehalose-poor regions. Importantly, since the phase separation process is associated with diffusion of excipients, the enhanced mobility in phase-separated T15L2 is expected to lower the activation energy barrier for crystal growth [49], which would not happen in T15. Therefore, we propose that the greater diffusion of excipients during phase separation is responsible for the higher rate of crystallization in Lutrol-containing samples compared to trehalose-only samples. This is supported by the observed positive correlation between the amount of phase separation and crystallization, as evidenced by XRD analysis (Figs. 2, 3, and 5).

The very low T_g values during drying suggests that plasticizing effects of water provided a thermodynamic driving force for trehalose crystallization in the trehalose/Lutrol coating during the drying process [50]. The plasticization effect was probably enhanced by the use of PBS [51], Additionally, CMC was shown to have a significant effect on the formulation's viscosity (Fig. S4). Since high viscosity is known to kinetically suppress molecular mobility and rearrangement, the addition of CMC would result in a decreased crystallization rate and could explain the lack of crystallization associated with CMC-containing samples during the early stage of the drying process [49, 52, 53].

4.4 Interfacial effects

The influence of Lutrol on the viral stability depended strongly on the surface properties of the Ti plates. As shown in Fig. 1b, HA activity decreased with increasing Lutrol concentration on plasma-cleaned Ti plates, but not on washed Ti plates. We also found that increasing Lutrol concentration increased phase transformations such as phase separation and crystallization of the vaccine coating on plasma-cleaned Ti plates using optical microscopy and XRD analysis (Figs. 2a(v)-(vii) and 2b(ii)).

In a separate study of the long-term stability of influenza vaccine-coated microneedles, the physicochemical properties of the vaccine coating were also found to be critical factors in determining protective immunogenicity of microneedles [15], Crystallization of trehalose in the vaccine coatings induced activity loss. Importantly, phase-separated samples with large bumps (>15 μm) exhibited a large decrease in functional HA activity, while samples with small bumps (< 15 μm) retained their full activity during storage. In our data (Fig 2a), the low-concentration (0.5%) Lutrol (which did not damage HA activity) had small bumps, whereas the higher concentration Lutrol formulations (which did damage HA activity) had large bumps, which appears consistent with previous findings.

As seen by optical micrographs and XRD analysis (Fig. 2), phase separation observed from the trehalose/Lutrol formulation was usually accompanied by crystallization. Based on this observation, it is not clear whether the phase transformations associated with the phase separation and/or the crystallization might be mechanistically responsible for loss of HA activity. However, such Lutrol-induced HA activity decrease was not seen in vaccine coatings on washed Ti plates (Fig. 4) that had little evidence of phase separation or crystallization (Figs. 5a(v)-(vii) and S2). In the case of the previous long-term stability test using the trehalose/Lutrol/CMC formulation, a drop in activity was seen in severely phase separated samples, even though the bumps were not crystallized (as measured by XRD), showing that phase-separation without crystallization could affect vaccine stability [15].

The enhanced stability of the vaccine coating on washed Ti plates can be explained in part by less phase transformation than on plasma-cleaned Ti plates (Figs. 5a(v)-(vii) and S2) possibly due to decreased nucleation of phase transformations on the washed Ti plate

surface. Another possibility is that the electrostatic/hydrophobic interactions of virus with the Ti substrate could be important in influencing stability of the vaccine during the drying process (discussed in section 3.4). The reactivity of Ti surfaces has been shown to play a critical role in protein adsorption behavior and to cause conformational changes in proteins [35-37], Thus, based on the observations of 1) the increase in wetting properties of Ti plates by plasma-cleaning, 2) the lower HA activity on plasma-cleaned Ti plates than on washed Ti plates, 3) the decrease in HA activity under more hydrophilic conditions (i.e., increase in Lutrol concentration), we propose that vaccine-metal substrate interactions occur more extensively on plasma-cleaned Ti plates (especially, in the presence of surfactant) due to the greater contact between the coating solution and Ti substrate, caused by easy spreading. Finally, it is worth noting that although trehalose/Lutrol coatings on washed Ti showed less phase transformation and less HA activity loss than on plasma-cleaned Ti microneedles, trehalose/Lutrol coatings on washed Ti microneedles were not immunogenic and performed just as badly as the coatings on plasma-cleaned Ti microneedles (Figs. 11 and 12). This inconsistency between *in vitro* HA assay and *in vivo* immunogenicity assay needs further study.

Questions remain as to why the addition of low concentrations of Lutrol better prevented the HA loss in trehalose-only coatings, possibly induced by osmotic pressure-driven effects (Figs. 1 and 4). A possible explanation is that the surfactant interacted with the viral envelope in a way that stabilized it against osmotic pressure-induced membrane perturbations. This is because Lutrol surfactant has been known to interact with liposomes or cell membranes through its penetration into lipid bilayers [54, 55]. However, our previous long-term stability tests showed that even small amounts of surfactant lead to phase separation eventually, even in the presence of CMC [15]. Thus, even though small amounts of surfactant might be a stabilizer in the short term, it is harmful in the long term. In the past, we have included surfactant in formulations to enable uniform coating of microneedle surfaces [9, 17], Here, we have shown that plasma cleaning is at least as effective at reducing contact angles as surfactant (Fig. 6) and thereby is expected to enable uniform coatings too. Additionally, plasma cleaning has no observable negative side effects on vaccine stability in coatings formulated without surfactant. While further research is needed to understand the mechanisms involved, from a practical point of view, formulations containing trehalose and surfactant do not appear suitable for microneedle coating with influenza vaccine.

4.5. Viscosity enhancer (CMC)

An important role of CMC, in addition to reducing osmotic pressure-driven effects, was to suppress phase transformations of the vaccine coating and possibly minimize the interaction of vaccine with the metal substrate, thereby enhancing vaccine stability during drying. The addition of CMC was found to significantly increase viscosity of the coating formulation (Fig. S4). Since crystallization and phase separation of vaccine coatings are driven by diffusion of excipients, a high viscosity can suppress these processes. Moreover, high viscosity can reduce the chance of virus interaction with the metal substrate. Our data consistently show that the addition of CMC to trehalose-only and trehalose/Lutrol formulations increases vaccine stability during drying (Figs, 1a, 4 and 7).

4.6. Coating microneedles

When we compared coatings on Ti plates to coatings on microneedles, all of the microneedles groups showed similar morphology to the Ti plates. Lutrol-induced phase separation was observed with the trehalose/Lutrol coating formulations on both washed and plasma-cleaned Ti microneedles. However, as shown in Figs. 10c and d, extensive phase separation was observed throughout the microneedle coatings, whereas the Ti plates showed

phase separation only over a more limited fraction of the coating. This may be because the drops applied to Ti sheets spread over a larger area of approximately 0.15 – 0.2 cm^2, whereas the coatings applied to microneedles were limited to the surface areas of the microneedles, which was about 3×10^{-3} cm^2 per microneedle. Because surfactant molecules are known to assemble along interfaces to minimize surface energy of the system [56], less surfactant is expected to assemble along the liquid-air and liquid-metal interfaces on microneedles than on the Ti plates. This can result in an increased surfactant concentration in the rest of coating. This increased surfactant concentration in the bulk coating may cause greater phase separation on microneedles than on Ti plates.

4.7. Immunogenicity

Little or no serum IgG antibody response was detected from the trehalose/Lutrol formulations on both washed and plasma-cleaned microneedles (Fig. 11), which is consistent with the 0% survival rate after challenge (Fig. 12). This can be explained by a decrease in vaccine efficacy due to phase transformation on Lutrol-containing microneedles (for both plasma-cleaned and washed) and affinity between vaccine and microneedle substrate (for plasma-cleaned). The high-concentration (2%) Lutrol formulations used in this study had phase separation with large bumps (>15 μm) and crystallization, which damages the vaccine. In addition, the trehalose/Lutrol/CMC group showed a higher level of antibody production and 100% protection against lethal viral challenge compared to the trehalose/Lutrol groups, probably because CMC functions to suppress phase transformation and vaccine-substrate interaction in the coating, which protects the vaccine.

4.8. Coating formulation recommendation

Based on these data generated using whole inactivated influenza virus vaccine, we recommend that a coating formulation should contain 15% trehalose to stabilize the vaccine during drying (based on prior literature [12, 19]); and CMC (less than 2%) or some other viscosity enhancer to reduce osmotic stress, suppress phase transformations, and minimize interactions between the vaccine and Ti metal plates. Formulations with Lutrol cause vaccine-destabilizing phase transformations during long-term storage, even in the presence of CMC [15], as well as a decrease in vaccine activity via interaction with plasma-cleaned metal substrates. If the coating is too hydrophobic to coat properly, plasma cleaning can be used to enhance the wettability of the microneedles. However, our data show that in the case of plasma cleaning, the coating formulation should not contain surfactant in order to reduce the vaccine destabilization due to adsorption onto metal substrate. If surfactants are used, it appears to be critical to modify the surface chemistry of the metal substrate after/during plasma treatment to prevent vaccine adsorption [57]. In addition, while our work has been performed using DPBS without calcium and magnesium, the possibilities of enhanced biomolecule-metal substrate interaction via bridging effects of divalent cations [58], pH changes during drying [59, 60], and PBS-induced T_g variation/crystallization [51] provide the need of further research on the effects of buffer composition on the stability of vaccine coated onto microneedles.

5. Conclusions

In this work, stability of influenza vaccine during coating onto microneedles was investigated. We examined the role of excipients used in current microneedle coating formulations, focusing on the stabilizing effect of sugar, osmotic pressure, phase transformations of the coating, and suitability of the coating formulation to coat microneedles. This work showed that 1) trehalose significantly protects influenza vaccine during drying, and that 2) osmotic pressure increase caused by high sugar concentration, phase transformation (i.e., phase separation and crystallization) of the vaccine coating, and

interactions between vaccine and metal substrates are vaccine-destabilizing factors affecting stability of the vaccine during coating. We further observed that the presence of a moderate amount of viscosity enhancer in the trehalose-only and trehalose/surfactant formulations had a strong stabilizing effect on the vaccine coating during drying by dampening osmotic pressure applied to the vaccine and suppressing phase transformation. We found that the surfactant Lutrol® micro 68 was a cause of phase separation of the coatings, and that this effect was enhanced on the plasma-cleaned metal substrate. Although the stability factors addressed in this study are limited and further research is needed, this study offers useful insight into mechanisms of vaccine damage during coating and presents guidelines to design formulations that preserve vaccine efficacy for influenza vaccine and other vaccines as well.

Supplementary Material

Refer to Web version on PubMed Central for supplementary material.

Acknowledgments

This project was primarily carried out at the Institute for Bioengineering and Bioscience and the Center for Drug Design, Development and Delivery at the Georgia Institute of Technology. Animal studies and associated analytic work were carried out at Emory University. This work was financially supported by NIH grants EB006369 (M.R.P.) and AI0680003 (R.W.C.), and AI093772 (S.M.K.) and AI087782 (S.M.K.). The authors acknowledge Donna Bondy for administrative support of this research, Dr. Seong-0 Choi and Dr. Jeong Woo Lee for help on *in vitro* reproducibility tests, James Norman for advisement on statistics, and AquaZ Inc (Cincinnati, OH) for allowing us to use their stopped-flow light scattering machine.

References

[1]. van der Maaden K, Jiskoot W, Bouwstra J. Microneedle technologies for (trans)dermal drug and vaccine delivery. J. Control. Release. 2012; 161:645–655. [PubMed: 22342643]

[2]. Al-Zahrani S, Zaric M, McCrudden C, Scott C, Kissenpfennig A, Donnelly RF. Microneedle-mediated vaccine delivery: harnessing cutaneous immunobiology to improve efficacy. Expert Opin. Drug Deliv. 2012; 9:541–550. [PubMed: 22475249]

[3]. Kim YC, Park JH, Prausnitz MR. Microneedles for drug and vaccine delivery. Adv. Drug Deliv. Rev. 2012 doi:10.1016/j.addr.2012.04.005.

[4]. Kim YC, Quan FS, Yoo DG, Compans RW, Kang SM, Prausnitz MR. Enhanced memory responses to seasonal H1N1 influenza vaccination of the skin with the use of vaccine-coated microneedles. J. Infect. Dis. 2010; 201:190–198. [PubMed: 20017632]

[5]. Chen X, Kask AS, Crichton ML, McNeilly C, Yukiko S, Dong L, Marshak JO, Jarrahian C, Fernando GJ, Chen D, Koelle DM, Kendall MA. Improved DNA vaccination by skin-targeted delivery using dry-coated densely-packed microprojection arrays. J. Control. Release. 2010; 148:327–333. [PubMed: 20850487]

[6]. Carey JB, Pearson FE, Vrdoljak A, McGrath MG, Crean AM, Walsh PT, Doody T, O'Mahony C, Hill AV, Moore AC. Microneedle array design determines the induction of protective memory CD8+ T cell responses induced by a recombinant live malaria vaccine in mice. PLoS One. 2011; 6:e22442. [PubMed: 21799855]

[7]. del Pilar Martin M, Weldon WC, Zarnitsyn VG, Koutsonanos DG, Akbari H, Skountzou I, Jacob J, Prausnitz MR, Compans RW. Local response to microneedle-based influenza immunization in the skin. MBio. 2012; 3:e00012–00012. [PubMed: 22396479]

[8]. Teunissen, MBM. Intradermal immunization. Springer-Verlag; Heidelberg ; New York: 2012.

[9]. Gill HS, Prausnitz MR. Coated microneedles for transdermal delivery. J. Control. Release. 2007; 117:227–237. [PubMed: 17169459]

[10]. Chen X, Prow TW, Crichton ML, Jenkins DW, Roberts MS, Frazer IH, Fernando GJ, Kendall MA. Dry-coated microprojection array patches for targeted delivery of immunotherapeutics to the skin. J. Control. Release. 2009; 139:212–220. [PubMed: 19577597]

[11]. Andrianov AK, DeCollibus DP, Gillis HA, Kha HH, Marin A, Prausnitz MR, Babiuk LA, Townsend H, Mutwiri G. Poly[di(carboxylatophenoxy)phosphazene] is a potent adjuvant for intradermal immunization. Proc. Natl. Acad. Sci. U. S. A. 2009; 106:18936–18941. [PubMed: 19864632]

[12]. Kim YC, Quan FS, Compans RW, Kang SM, Prausnitz MR. Formulation and coating of microneedles with inactivated influenza virus to improve vaccine stability and immunogenicity. J. Control. Release. 2010; 142:187–195. [PubMed: 19840825]

[13]. Ameri M, Fan SC, Maa YF. Parathyroid hormone PTH(1-34) formulation that enables uniform coating on a novel transdermal microprojection delivery system. Pharm. Res. 2010; 27:303–313. [PubMed: 20013035]

[14]. Jameel, F.; Hershenson, S. Formulation and process development strategies for manufacturing biopharmaceuticals. Wiley; Hoboken, N.J.: 2010.

[15]. Choi HJ, Yoo DG, Bondy BJ, Quan FS, Compans RW, Kang SM, Prausnitz MR. Stability of influenza vaccine coated onto microneedles. Biomaterials. 2012; 33:3756–3769. [PubMed: 22361098]

[16]. Amorij J-P, Huckriede A, Wilschut J, Frijlink HW, Hinrichs WLJ. Development of stable influenza vaccine powder formulations: challenges and possibilities. Pharm. Res. 2008; 25:1256–1273. [PubMed: 18338241]

[17]. Gill HS, Prausnitz MR. Coating formulations for microneedles. Pharm. Res. 2007; 24:1369–1380. [PubMed: 17385011]

[18]. Crowe JH, Hoekstra FA, Crowe LM. Anhydrobiosis. Annu. Rev. Physiol. 1992; 54:579–599. [PubMed: 1562184]

[19]. Quan FS, Kim YC, Yoo DG, Compans RW, Prausnitz MR, Kang SM. Stabilization of influenza vaccine enhances protection by microneedle delivery in the mouse skin. PLoS One. 2009; 4:e7152. [PubMed: 19779615]

[20]. Stanekova Z, Vareckova E. Conserved epitopes of influenza A virus inducing protective immunity and their prospects for universal vaccine development. Virol. J. 2010; 7:351. [PubMed: 21118546]

[21]. Novak M, Moldoveanu Z, Schafer DP, Mestecky J, Compans RW. Murine model for evaluation of protective immunity to influenza virus. Vaccine. 1993; 11:5560.

[22]. Hirst GK. The quantitative determination of influenza virus and antibodies by means of red cell agglutination. J. Exp. Med. 1942; 75:49–64. [PubMed: 19871167]

[23]. Shah B, Kakumanu VK, Bansal AK. Analytical techniques for quantification of amorphous/crystalline phases in pharmaceutical solids. J. Pharm. Sci. 2006; 95:1641–1665. [PubMed: 16802362]

[24]. Quan FS, Huang C, Compans RW, Kang SM. Virus-like particle vaccine induces protective immunity against homologous and heterologous strains of influenza virus. J. Virol. 2007; 81:3514–3524. [PubMed: 17251294]

[25]. Elversson J, Millqvist-Fureby A. In situ coating-an approach for particle modification and encapsulation of proteins during spray-drying. Int. J. Pharm. 2006; 323:52–63. [PubMed: 16887302]

[26]. Taga T, Senma M, Osaki K. The crystal and molecular structure of trehalose dihydrate. Acta Cryst. B. 1972; 28:3258–3263.

[27]. Nagase H, Ogawa N, Endo T, Shiro M, Ueda H, Sakurai M. Crystal structure of an anhydrous form of trehalose: structure of water channels of trehalose polymorphism. J. Phys. Chem. B. 2008; 112:9105–9111. [PubMed: 18605683]

[28]. Mattox DM. Surface cleaning in thin film technology, thin solid films. 1978; 53:81–96.

[29]. O'Kane DF, Mittal KL. Plasma cleaning of metal surfaces. J. Vac. Sci. Technol. 1974; 11:567–569.

[30]. Tengvall P, Lundström I. Physico-chemical considerations of titanium as a biomaterial. Clin. Mater. 1992; 9:115–134. [PubMed: 10171197]

[31]. Barin, I.; Knacke, O. Thermochemical properties of inorganic substances. Springer-Verlag; Berlin, Germany: 1973.

[32]. Brunette, DM.; Tengvall, P.; Textor, M.; Thomsen, P. Titanium in medicine: material science, surface science, engineering, biological responses, and medical applications. Springer-Verlag; Berlin ; Heidelberg: 2001. p. 171-230.p. 457-512.

[33]. Berberich LJ, Bell ME. The dielectric properties of the rutile form of titanium dioxide. J. App. Phys. 1940; 11:681–692.

[34]. Parks GA. The isoelectric points of solid oxides, solid hydroxides, and aqueous hydroxo complex systems. Chem. Rev. 1965; 65:177–198.

[35]. Ivarsson BA, Hegg PO, Lundstrom KI, Jonsson U. Adsorption of proteins on metal-surfaces studied by ellipsometric and capacitance measurements. Colloids Surf. 1985; 13:169–192.

[36]. Wassell DTH, Embery G. Adsorption of bovine serum albumin on to titanium powder. Biomaterials. 1996; 17:859–864. [PubMed: 8718930]

[37]. Liedberg B, Ivarsson B, Lundstrom I. Fourier transform infrared reflection absorption spectroscopy (FT-IRAS) of fibrinogen adsorbed on metal and metal oxide surfaces. J. Biochem. Biophys. Methods. 1984; 9:233–243. [PubMed: 6470402]

[38]. Oleson TA, Sahai N. Oxide-dependent adsorption of a model membrane phospholipid, dipalmitoylphosphatidylcholine: bulk adsorption isotherms. Langmuir. 2008; 24:4865–4873. [PubMed: 18348581]

[39]. Rabe M, Verdes D, Seeger S. Understanding protein adsorption phenomena at solid surfaces. Adv. Colloid. Interface Sci. 2011; 162:87–106. [PubMed: 21295764]

[40]. Brown AD. Microbial water stress. Bacteriol. Rev. 1976; 40:803–846. [PubMed: 1008746]

[41]. Loeb J. The reciprocal relation between the osmotic pressure and the viscosity of gelatin solutions. J. Gen. Physiol. 1921; 4:97–112. [PubMed: 19871918]

[42]. Kunitz M. An empirical formula for the relation between viscosity of solution and volume of solute. J. Gen. Physiol. 1926; 9:715–725. [PubMed: 19872286]

[43]. Borgnia MJ, Kozono D, Calamita G, Maloney PC, Agre P. Functional reconstitution and characterization of AqpZ, the E. coli water channel protein. J. Mol. Biol. 1999; 291:1169–1179. [PubMed: 10518952]

[44]. Gordon M, Taylor JS. Ideal copolymers and the second-order transitions of synthetic rubbers. i. non-crystalline copolymers. J. Appl. Chem. 2007; 2:493–500.

[45]. Chen T, Fowler A, Toner M. Literature review: supplemented phase diagram of the trehalose-water binary mixture. Cryobiology. 2000; 40:277–282. [PubMed: 10860627]

[46]. Bhat SN, Sharma A, Bhat SV. Vitrification and glass transition of water: insights from spin probe ESR. Phys. Rev. Lett. 2005; 95:235–702.

[47]. Telang C, Yu L, Suryanarayanan R. Effective inhibition of mannitol crystallization in frozen solutions by sodium chloride. Pharm. Res. 2003; 20:660–667. [PubMed: 12739776]

[48]. Roos YH. Characterization of food polymers using state diagrams. J. Food Eng. 1995; 24:339–360.

[49]. Turnbull D, Fisher JC. Rate of nucleation in condensed systems. J. Chem. Phys. :17.

[50]. Ding SP, Fan J, Green JL, Lu Q, Sanchez E, Angell CA. Vitrification of trehalose by water loss from its crystalline dihydrate. J. Therm. Anal. 1996; 47:1391–1405.

[51]. Sitaula R, Bhowmick S. Moisture sorption characteristics and thermophysical properties of trehalose-pbs mixtures. Cryobiology. 2006; 52:369–385. [PubMed: 16545359]

[52]. Karmas R, Pilar Buera M, Karel M. Effect of glass transition on rates of nonenzymic browning in food systems. J. Agric. Food Chem. 1992; 40:873–879.

[53]. Yoshioka S, Aso Y, Kojima S. The effect of excipients on the molecular mobility of lyophilized formulations, as measured by glass transition temperature and NMR relaxation-based critical mobility temperature. Pharm. Res. 1999; 16:135–140. [PubMed: 9950292]

[54]. Lee RC, Myerov A, Maloney CP. Promising therapy for cell membrane damage. Ann. N. Y. Acad. Sci. 1994; 720:239–245. [PubMed: 8010645]

[55]. Wu G, Majewski J, Ege C, Kjaer K, Weygand MJ, Lee KY. Interaction between lipid monolayers and poloxamer 188: an x-ray reflectivity and diffraction study. Biophys. J. 2005; 89:3159–3173. [PubMed: 16100276]

[56]. Starov, VM.; Velarde, MG.; Radke, CJ. Wetting and spreading dynamics. CRC Press; 2007.

[57]. Liu X, Chu PK, Ding C. Surface modification of titanium, titanium alloys, and related materials for biomedical applications. Mater. Sci. Eng. 2004; R47:49–121.

[58]. Ellingsen JE. A study on the mechanism of protein adsorption to TiO_2. Biomaterials. 1991; 12:593–596. [PubMed: 1663394]

[59]. Amorij JP, Meulenaar J, Hinrichs WL, Stegmann T, Huckriede A, Coenen F, Frijlink HW. Rational design of an influenza subunit vaccine powder with sugar glass technology: preventing conformational changes of haemagglutinin during freezing and freeze-drying. Vaccine. 2007; 25:6447–6457. [PubMed: 17673338]

[60]. Saluja V, Amorij JP, Kapteyn JC, de Boer AH, Frijlink HW, Hinrichs WL. A comparison between spray drying and spray freeze drying to produce an influenza subunit vaccine powder for inhalation. J. Control. Release. 2010; 144:127–133. [PubMed: 20219608]

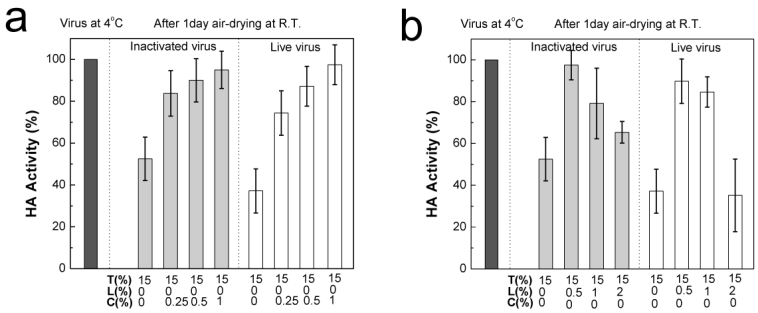

Fig. 1.

Effect of coating formulations on functional HA activity of influenza virus after drying on plasma-cleaned Ti plates. The effects of viscosity enhancer (CMC) (a) and surfactant (Lutrol) (b) on the activity of inactivated influenza virus and live influenza virus were investigated by measuring HA titers at three different CMC concentrations (0.25%, 0.5%. 1%) and three different Lutrol concentrations (0.5%, 1%, 2%) with 15% trehalose. Inactivated and live A/PR/8/34 virus (1 μg of viral protein) coatings were prepared on plasma-cleaned Ti plates and dried at ambient conditions (20 – 23 °C, 20 – 45% relative humidity) for one day. HA activity change was calculated with respect to HA titer of the virus in DPBS solution. Unless otherwise indicated, all measurements were performed at 4 °C. Data are represented as the mean ± standard deviation (SD) from $n = 8 – 23$ replicates.

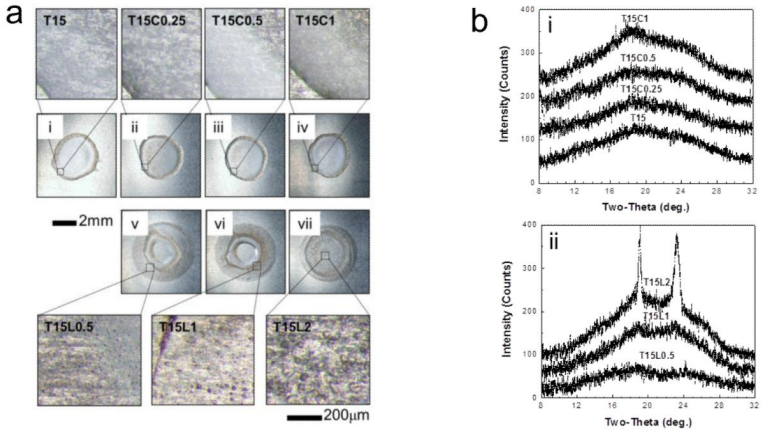

Fig. 2.

Phase transformations in coatings containing CMC or Lutrol on plasma-cleaned Ti plates, (a) Brightfield optical microscopy images of vaccine coatings on Ti plates. Coating samples with 1 μg of virus protein were prepared at room temperature and micrographs were taken after incubation at room temperature for one day. Micrographs (i)-(vii) represented in (a) were obtained by monitoring the morphological changes of the same samples as shown in Fig. 1. Coating formulations were as follows: (i) T15; (ii) T15C0.25; (iii) T15C0.5; (iv) T15C1; (v) T15L0.5; (vi) T15L1; (vii) T15L2. The magnified images (below) show the typical morphology of phase-separated samples with bumps in images (v)-(vii). Images are representative of $n = 6$ replicate samples examined at each condition, (b) X-ray diffraction (XRD) patterns corresponding to (i)-(vii) shown in part (a), (i) XRD spectra measured from T15, T15C0.25, T15C0.5, and T15C1 coatings, (ii) XRD spectra measured from coating formulations containing T15L0.5, T15L1 and T15L2. Structural analysis was performed by comparing observed characteristic XRD peaks with simulation results based on cell information of trehalose-dihydrate and trehalose anhydrous forms [27]. XRD patterns observed from T15L1 and T15L2 contain characteristic peaks for crystalline trehalose-dihydrate. The intensity of crystalline peaks increased with increasing Lutrol concentration. This indicates that trehalose crystallization is enhanced by the presence of Lutrol in the vaccine coating formulation. Magnified XRD spectra corresponding to T15L1 and T15L2 can be found in Fig. SI together with the percent crystallinity. Spectra are representative of $n = 6$ replicate samples examined at each condition.

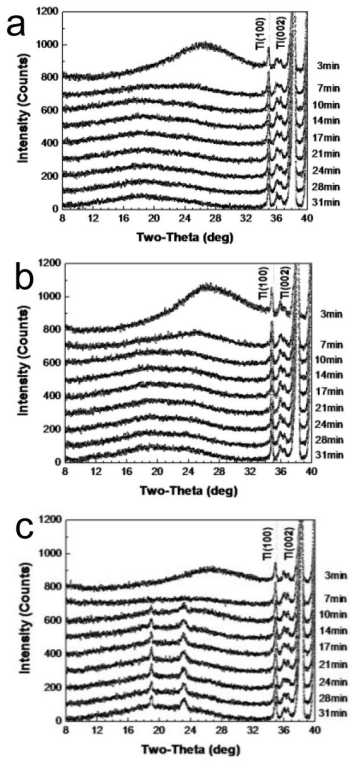

Fig. 3.

Time-dependant x-ray diffraction spectra over time during drying after coating on plasma-cleaned Ti plates at room temperature for (a) T15, (b) T15C1, and (c) T15L2 formulations. Drying times are indicated at the right side of each curve. Peaks on the right part of the spectra (Ti(100), Ti(002)) represent the titanium plate. The vaccine-embedded coating formulation with T15L2 began to crystallize within 10 min upon drying. Spectra are representative of $n = 6$ replicate samples examined at each condition.

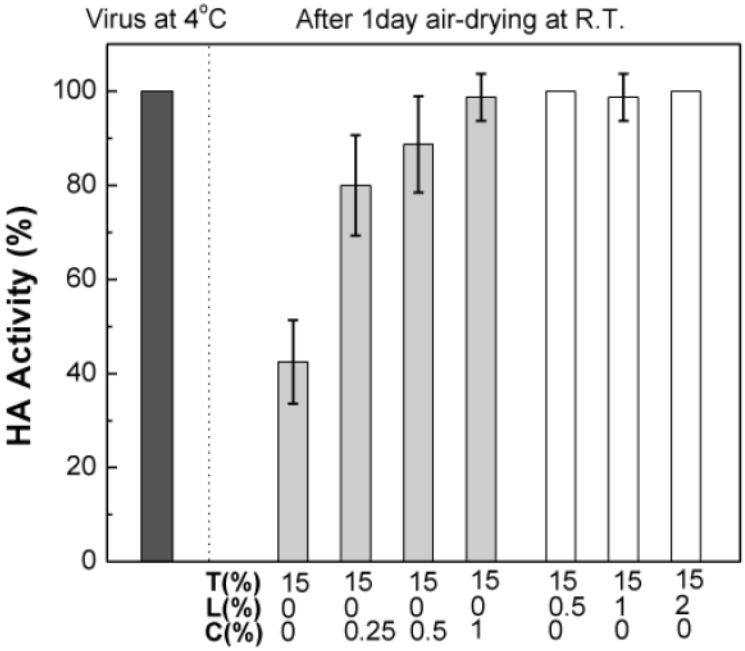

Fig. 4.

Effect of coating formulation on the functional HA activity of inactivated influenza virus after diying on washed Ti plates. The effects of CMC and Lutrol on the activity of the influenza virus (1 μg viral protein) were investigated by measuring HA titers in different vaccine coating formulations after one day drying at ambient conditions: T15, T15C0.25, T15C0.5, T15C1, T15L0.5, T15L1, and T15L2. (Mean ± SD; $n = 16$)

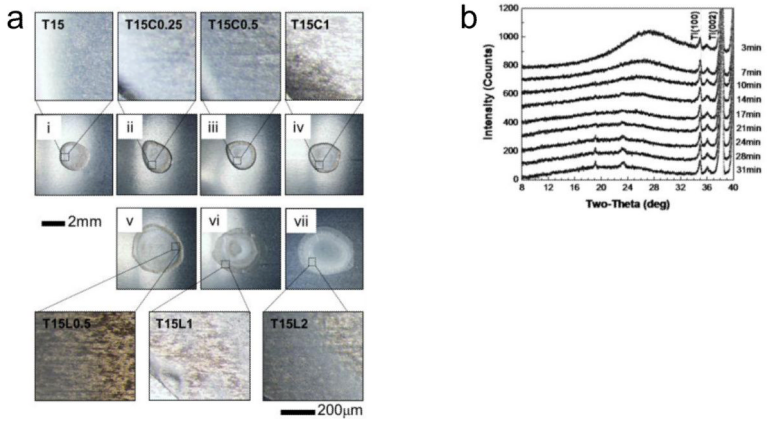

Fig. 5.

Phase transformations in coatings containing CMC or Lutrol on washed Ti plates, (a) Brightfield optical microscopy images for vaccine coating samples on Ti plates. The same conditions were used as in Fig. 2a except for the Ti plate cleaning method. Micrographs (i)-(vii) were obtained by monitoring the morphological changes of the same samples as in Fig. 4. Coating formulations were: (i) T15; (ii) T15C0.25; (iii) T15C0.5; (iv) T15C1; (v) T15L0.5; (vi) T15L1; (vii) T15L2. The magnified images (below) (v) – (vii) indicate phase separation similarly to Fig. 2a. Images are representative of $n = 6$ replicate samples examined at each condition, (b) Time-dependant x-ray diffraction spectra measured during drying of vaccine coated in T15L2 formulation on a washed Ti plate at room temperature. Drying times are indicated at the right side of each curve. Peaks on the right part of the spectra (Ti(100), Ti(002)) represent the titanium plate. The XRD spectra show that vaccine coating begins to crystallize within 14 min upon drying. Spectra are representative of $n = 3$ replicate samples examined at each condition.

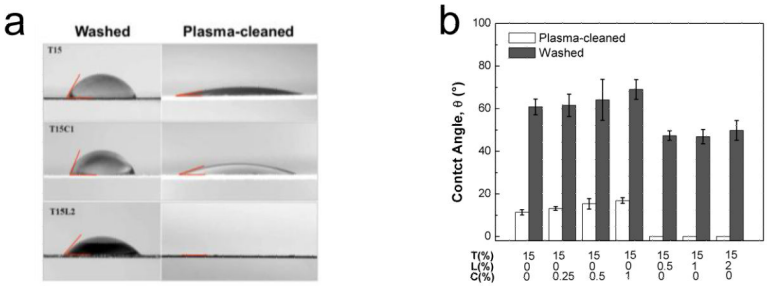

Fig. 6.

Contact angle measurements. (a) Optical micrographs showing the contact angle between a droplet of coating formulation and Ti plates. Images correspond to representative T15, T15C1, and T15L2 formulations on washed and plasma-cleaned Ti plates. (b) Relationship between composition of coating formulation and contact angle on washed and plasma-cleaned Ti plates. Vaccine coating formulations showed better wetting on plasma-cleaned Ti plates than on washed Ti plates. Samples containing Lutrol provided better and complete wetting on washed and plasma-cleaned Ti plates, respectively. (Mean ± SD; $n = 6$)

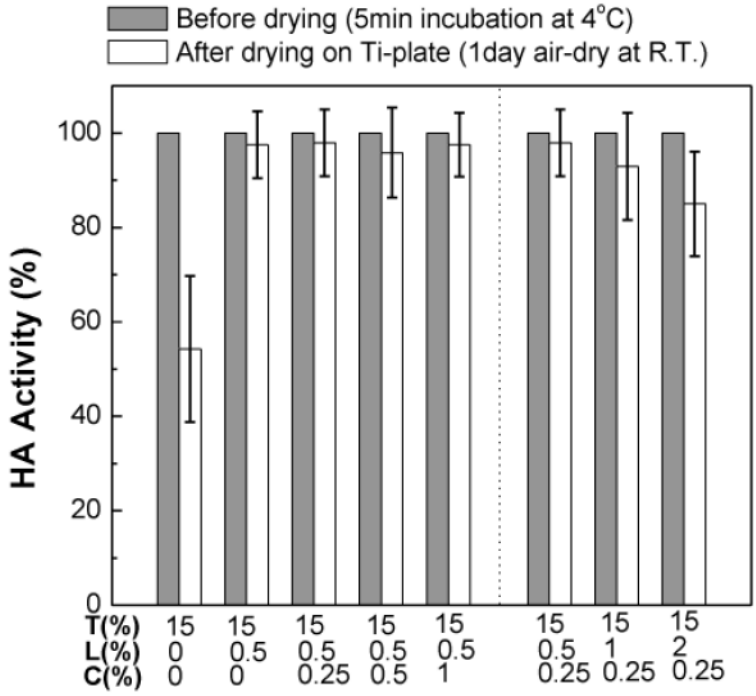

Fig. 7.

Stabilizing effect of viscosity enhancer on the functional HA activity of dried vaccine coatings on plasma-cleaned Ti plates with formulations containing both Lutrol and CMC. The effects of viscosity enhancer (CMC) on the activity of the influenza viruses (1 μg viral protein) were investigated by measuring HA titers in different vaccine coating formulations after one day drying at ambient conditions. CMC concentration was varied at fixed trehalose/Lutrol concentration (T15L0.5C0.25, T15L0.5C0.5, T15L0.5C1) and Lutrol concentration was varied at fixed trehalose/CMC concentration (T15L0.5C0.25, T15L1C0.25, T15L2C0.25). (Mean ± SD; $n = 8 – 23$)

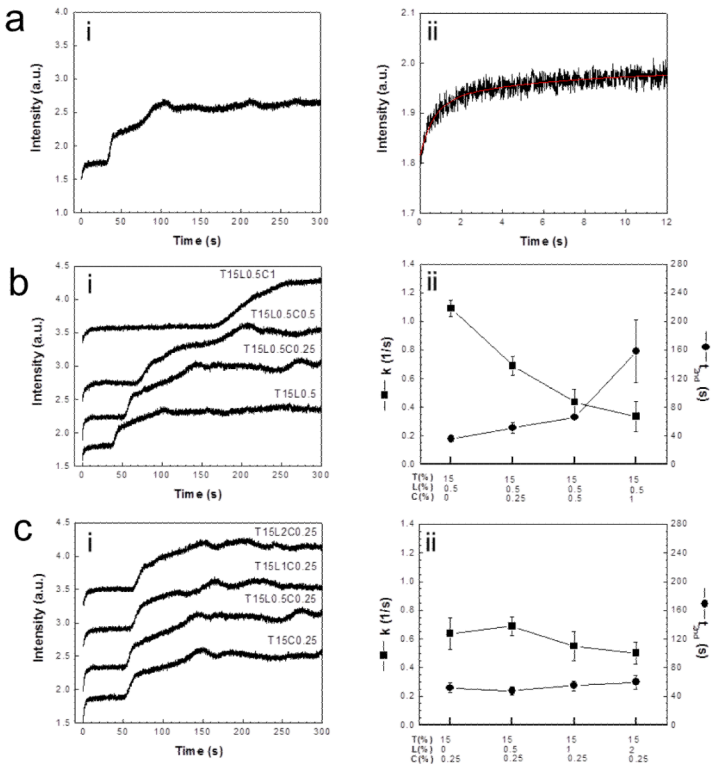

Fig. 8.

SFLS analysis of inactivated virus incubated in different coating formulations: (a) trehalose-only (T15), (b) various CMC concentrations at fixed trehalose/Lutrol concentration (T15L0.5, T15L0.5C0.25, T15L0.5C0.5, T15L0.5C1) and (c) various Lutrol concentrations at fixed trehalose/CMC concentration (T15C0.25, T15L0.5C0.25, T15L1C0.25, T15L2C0.25). Virus suspensions (0.2 mg/ml) were abruptly placed in hyperosmotic coating formulation solutions in a stopped-flow apparatus and the resulting changes in scattered light intensity were monitored at 546 nm as a function of time for 12 s and 300 s (i). The rate constant (k [1/s]) for primary shrinkage and onset time for secondary shrinkage (t_{2nd} [s]) were determined from single exponential curve fit to the 12-s scan data [43] and the spectral curve analysis of the 300-s scan data, respectively (i). Exponential curve fitted to the 12-s SFLS curve in response to hyperosmotic gradient by T15 formulation is shown in a(ii) as a representative example ($k = 1.04 \pm 0.14\ s^{-1}$, $t_{2nd} = 34.4 \pm 7.0$ s). Rate constants and onset time for secondaiy shrinkage are plotted for different coating formulations tested (ii).

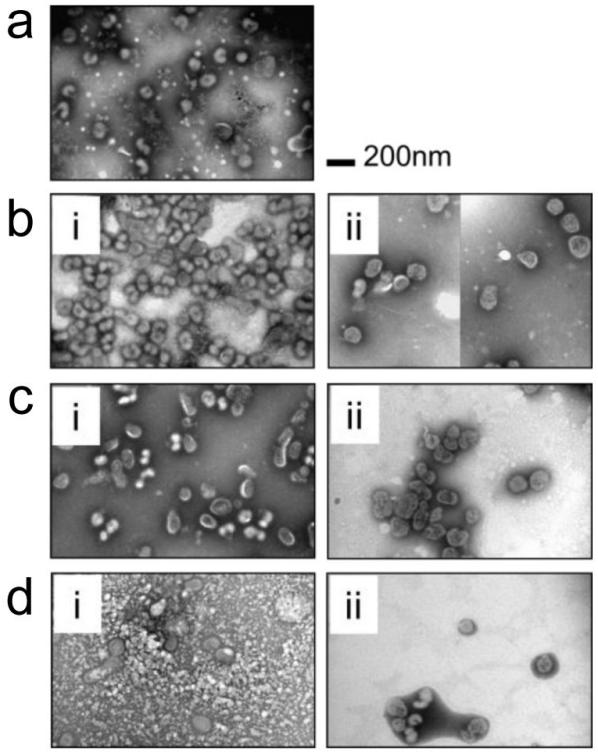

Fig. 9.

TEM images of inactivated virus, (a) in DPBS at 4 °C, (b) in T15L0.5C0.25 formulation (i) incubated for 5 min at 4 °C and (ii) in a solid coating dried for one day. (c) in T15L0.5C1 formulation (i) incubated for 5 min at 4 °C and (ii) in a solid coating dried for one day and (d) in T15L2C0.25 formulation (i) incubated for 5 min at 4°C and (ii) in a solid coating dried for one day. Vaccine-embedded coatings were prepared on plasma-cleaned Ti plates. After drying, solid coating was dissolved in DPBS and vaccine sample was transferred on copper grid for TEM observation. TEM analysis shows that none of the solid coating formulations induce morphological change of the virus after diying for one day, despite phase separations. It is noted that differences in the appearance of the TEM images are due to the interaction of the staining solution with the coating formulation excipients.

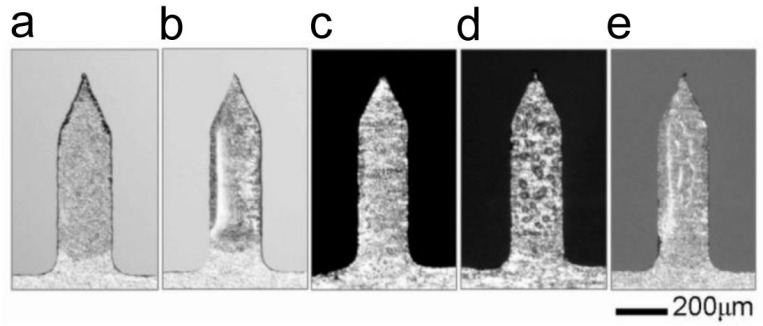

Fig. 10.

Five groups of vaccine-coated Ti microneedles with inactivated A/PR/8/34 influenza virus. Plasma-cleaned Ti microneedles were used for coating formulations with (a) T15, (b) T15C1, and (c) T15L2 formulations. For comparison, washed Ti microneedles were separately used for (d) with a T15L2 formulation. To see the effect of CMC addition to T15L2, microneedles were prepared in (e) using a T15L2C1 formulation. Influenza vaccine-coated microneedles with 0.12 μg of protein were air-dried for one day at ambient conditions. Images shown in (c) and (d) indicate the presence of phase separation in both washed and plasma-cleaned Ti microneedles with T15L2. However, as shown in (e). morphological change of the dried vaccine coating was suppressed due to the addition of CMC to the coating formulation. Images are representative of $n = 10$ replicate samples examined at each condition.

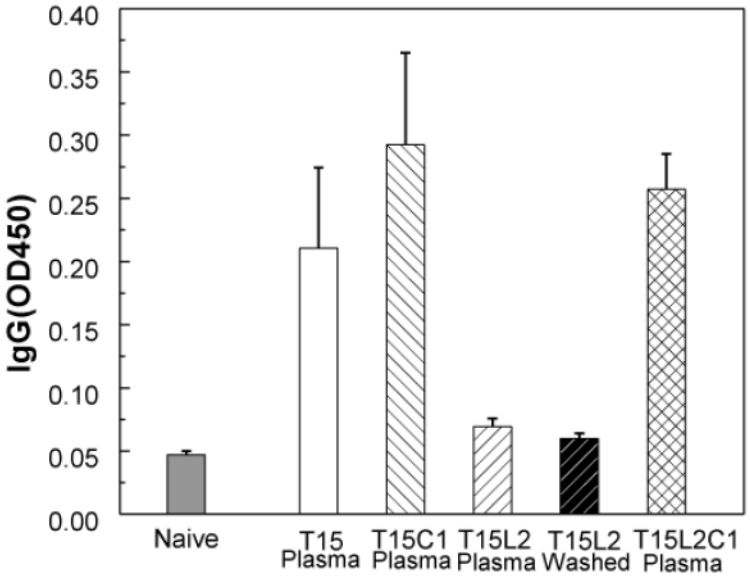

Fig. 11.

Comparison of antibody responses after immunization using vaccine-coated microneedles. Total serum anti-A/PR/8/34 IgG levels were determined by reading optical densities using ELISA. IgG was measured from mice bled on the 2nd week following immunization (0.12 μg of viral protein). (Mean ± SD, $n = 6$ mice per group)

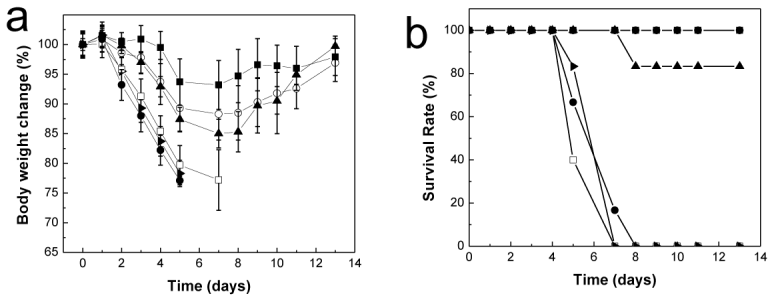

Fig. 12.

Protection of immunized mice against lethal challenge, (a) Body weight changes, (b) Survival rates. At week 4 after vaccination, groups of mice were intranasally challenged with 10×LD_{50} of mouse-adapted A/PR/8/34 virus. Body weight changes and survival rates were monitored daily and recorded for 13 days. Naïve (●), T15 (plasma-cleaned, ▲), T15C1 (plasma-cleaned, ○), T15L2 (plasma-cleaned, □), T15L2 (washed, ▶), and T15L2C1 (plasma-cleaned, ■). (Mean ± SD, $n = 6$)